

# Spectroscopic Properties of the Interaction between Chlorophyll and Agrochemicals

Leonardo Marmo Moreira<sup>a</sup>, Jane de Moraes Ramos<sup>b</sup>, Hueder Paulo Moisés de Oliveira<sup>c</sup>, and Ana Paula Romani<sup>d,\*</sup>

<sup>a</sup>Universidade Federal de São João Del Rei, Departamento de Zootecnia (DEZOO). Campus CTAN, Fábricas, São João Del Rei, 36301-160, Minas Gerais, Brazil.

<sup>b</sup>Universidade Federal de Ouro Preto / Escola de Farmácia. Morro do Cruzeiro s/n. Bairro Bauxita – CEP 35400-000, Ouro Preto, Minas Gerais, Brazil.

<sup>c</sup>Universidade Federal do ABC / Centro de Ciências Naturais e Humanas. Avenida dos Estados, 5001. Bairro Bangu - CEP 09210-580, Santo André, São Paulo, Brazil.

<sup>d</sup>Universidade Federal do ABC / Centro de Engenharia, Modelagem e Ciências Sociais Aplicadas. Avenida dos Estados, 5001. Bairro Bangu - CEP 09210-580, Santo André, São Paulo, Brazil.

*Article history:* Received: 01 April 2018; revised: 27 June 2018; accepted: 29 August 2018. Available online: 25 September 2018. DOI: <http://dx.doi.org/10.17807/orbital.v10i6.1160>

## Abstract:

The present work is focused on spectroscopic evaluations, employing optical absorption and fluorescence emission spectroscopies of chlorophylls and chlorophilic derivatives as well as the complex chemical systems originated by the interaction between chlorophyll compounds and agrochemicals, such as pesticides and insecticides. Considering the great variation of chlorophyll compounds that can be encountered in each plant species as well as the high number of agrochemicals that are frequently used in the agriculture, this approach can be considered a relevant contribution to understand some mechanisms of chemical interaction and toxicological risks inherent to the chlorophyll-pesticides and chlorophyll-insecticides systems. This work also demonstrates that the high coefficient of molar absorptivity of chlorophyll as well as its great level of spectral details in terms of absorption bands can be employed as a model system to evaluate the intensity of contamination of plants with agrochemicals. This manuscript represents a multi- and interdisciplinary study, which is highly relevant to professionals and researchers of several distinct areas of knowledge. The results obtained are discussed in details, demonstrating that time-resolved fluorescence measurements are able to analyze the photophysical processes that involve chlorophylls, agrochemicals and the complex chemical systems formed by the interaction between chlorophylls and these compounds of high toxicity.

**Keywords:** chlorophyll; agrochemicals; agrochemical contamination; fluorescence spectroscopy

## 1. Introduction

The chlorophylls are the natural pigments of highest concentration in plants, being present in the chloroplasts of leaves and other plant tissues. The name “chlorophyll” was proposed by Pelletier and Caventou at 1818 to define the green substance that could be extracted of the leaves with alcohol [1]. They are macrocyclic compounds that present the cation  $Mg^{2+}$  as coordination center of the chlorine ring. These compounds present a significant structural flexibility and a relatively great tail that are chemical characteristics that affect intensely the reactivity of these compounds. Furthermore, the different

types of chlorophyll, which can coexist in several concentrations, depending on the plant species in which this compound is found, becomes the “group of chlorophilic compounds” a chemical system of significant variation in terms of chemical properties. This variation of chemical environments that have chlorophylls also increases the complexity of their studies, since it can be observed modification of the chemical reactivity; depending on the combination of the present chlorophyll types. This context reinforces the necessity of studies involving chlorophylls in model systems, to the respective physico-chemical profile can be identified from some information related to the polarity and/or apolarity

\*Corresponding author. E-mail: [ana.romani@ufabc.edu.br](mailto:ana.romani@ufabc.edu.br)

of the chemical environment, between other properties of the biological medium that present these chlorine compounds [1].

The great biological relevance of chlorophyll, which presents central role in the photosynthesis, presents several nuances that should be more explored in the literature. Indeed, the chlorophyll is compound inherent to various plants largely employed as food, implying that the peculiar chemical interactions of chlorophyll are relevant not only to the study of the biological chemistry inherent to the plant life, but equally to the animal biological systems and their respective nutrition processes. The roles of the chlorophyll in the human food as well as in various therapeutic applications, such as possible antioxidant, antimutagenic and chemopreventive activities are not yet well established in the literature [1]. On the other hand, one of the more detailed studies focused on the interaction between chlorophyll and agrochemicals consists in a relevant contribution to several multidisciplinary areas, since the systematic use of pesticides and insecticides has generated direct and indirect effects upon the own plants and, consequently, animals that use vegetables as food [2, 3].

Similarly, to the surface active agents (surfactants) of low molecular mass, various copolymers of block produce aggregates of different types, depending on the molecular mass, block sizes, solvent composition and temperature. In lower concentrations, frequently, it is observed the formation of micelles, while in higher concentrations can occur one liquid-crystalline phase [4]. The block copolymers are constituted of hydrophobic and hydrophilic blocks and, in the case of the micelle formation, the first one will constitute the nucleus and the last one in contact with the aqueous medium will originate the micelle outer layer [5]. Hydrophobic molecules can be incorporated in the nucleus of the polymeric micelle during the micelle formation. Considering the capability of micelles to transport lipophilic substances in aqueous medium, it is possible to correlate structural and functional similarities between micelles and plasma lipoproteins. Thus, when the micelles are formed by biocompatible copolymers, the polymeric micelles can act as a long-term loading system for hydrophobic molecules [6].

In the present days, the use of pesticides and

insecticides is still the main strategy to the prevention of agricultural pests, ensuring great availability and quality of food for the population, through higher animal and vegetal productions. However, these agrochemical compounds present potential toxicity to the human being and other several animal species, and can provoke prejudicial effects to the central and peripheral nervous systems, cause immunosuppressive effects and/or carcinogenic actions, between other effects [7]. Moreover, they can originate direct and indirect environmental contaminations. In spraying, pesticides wastes can be higher than 70% of the total of the product applied in the vegetal culture. It was verified losses between 30% and 50%, but, in some cases, the deposition in the plants has been superior to 64% of the total applied [8]. Aquatic bodies near the plantation areas are contaminated through runoff. The percolation of pesticide residues in the soil has also reached the groundwater, decreasing the quality of these waters. Effluents from the pesticide manufacturing industries are also responsible for environmental contamination [6].

When pesticides and/or insecticides are sprayed on culture fields, they may evaporate or be drawn into the soil by rain or irrigation water. In soil, these agrochemicals can be degraded by light, heat, interaction with soil particles, bacteria or other factors, giving rise to harmless waste, between other possibilities. Organic compounds applied as agrochemicals and their respective cleavage products can be transported on the surface of rivers, or retained and absorbed by soils. In the latter case, these pollutants can seep into the water table, contaminating sources of drinking water. Therefore, the real possibility of contamination of water and food with these products becomes it essential to monitor them at environmental levels, as well as the production of their respective derivatives. Thus, the constant evaluation of these species and their degradation products, which can present higher toxicity than their precursors, in the different matrix, is necessary procedure, justifying the efforts realized to the development of techniques and suitable analytical methods. These methodologies are adequate to improve the analysis time and sensitivity of the agrochemical determination in these matrices, as well as the possibility of application *in situ* in the agriculture [9].

In this way, the use of micelles and polymeric aggregated would be an alternative system to the controlled liberation of agrochemical compounds (herbicides, insecticides etc.). The efficiency of micelles and polymeric aggregates as systems that transport agrochemical products can be evaluated with fluorescence spectroscopy. When the plants are exposed to an environmental or biotic stress, it is possible to observe simultaneously alterations in the functional state of the membranes of the thylakoids from chloroplasts, provoking changes in the characteristics of the intrinsic fluorescence signals, which can be quantified in the leaves. Thus, agrochemicals can inhibit photosynthesis through the blocking of the electron transport in the photosystem and, in this way, decreasing the chlorophyll fluorescence. The analysis of the fluorescence emission kinetics of the chlorophylls allows the study of the properties related to the ability of absorption and energy transfer in the electron transport chain. In fact, it is possible to develop evaluations regarding the conformational changes of thylakoids as well as an increase in the knowledge of the photophysical processes that occur in the respective membranes of thylakoids inserted in the chloroplasts. This is a sensitive and non-destructive method, which, through the chlorophyll fluorescence, furnishes rapid information upon the processes in the photosynthetic apparatus. Consequently, data regarding the plant physiological state constitute an important tool to the investigation of the applied and basic physiologies [10-13].

In this work, it is analyzed the interaction between chlorophylls and different types of compounds with great relevance with respect to chemistry, biochemistry, environmental science and agriculture. Moreover, this study can contribute to the areas of animal and human nutrition, including pre-requisites to researchers of the health area that are focused on toxicological problems, such as contamination and fixation of agrochemical compounds, which have been studied in the context of the work medicine, between others.

## 2. Results and Discussion

### 2.1 Formation of polymeric micelles

After preparation of the polymer micelles

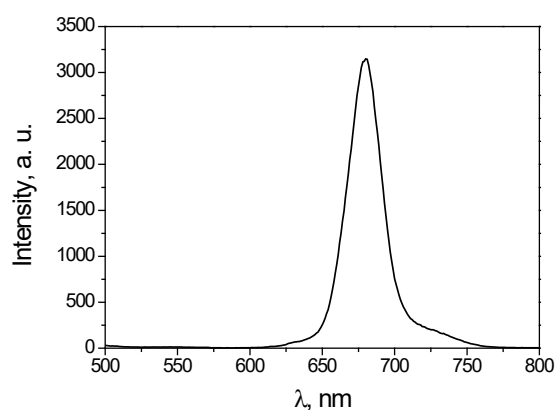
solution, a fluorescence emission experiment was performed in the presence of these structures. For this, pyrene was used as a fluorescent probe. Among the characteristics that make it suitable for studies in the presence of micelles can be cited [14]: a) long fluorescence lifetime, b) low solubility in water and high solubility in micellar systems, c) vibrational bands well resolved, and d) sensibility of these vibrational bands to the solvent. A stock solution of pyrene in methanol (spectroscopic grade) was prepared and an aliquot of that solution was added to the micellar solution. Then, the emission spectrum was recorded.

### 2.2 Spectroscopic properties of chlorophyll

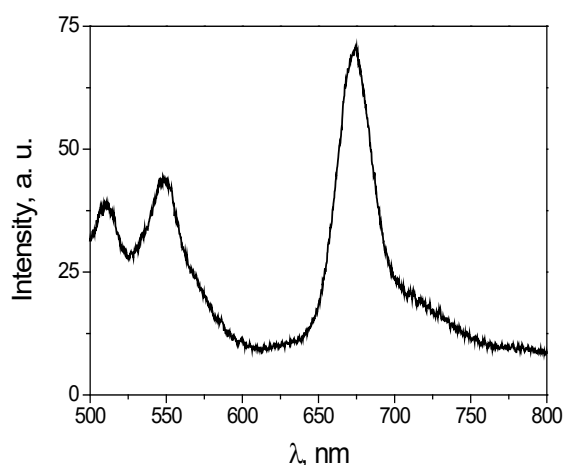
The spectral characteristics of the molecules are dependent on the solvent polarity and the local environment. The main factors that affecting the spectral properties are: solvent polarity and viscosity, solvent relaxation velocity, conformational changes of the probe, local environment rigidity, charge transfer, proton transfer and excited state reactions, interactions between probe molecules, interactions between solvent and probe molecules, variations in radiative and nonradiative decay rates. Chlorophyll **a** has electron-donor groups (methyl and ethyl) at positions 7 and 8 of its main ring. These groups impose an electron density, from the opposite sides of the molecule along the X axis, in the pyrrole nitrogens, which partially protect the charge of the metallic center of coordination of chlorophyll, i.e., the divalent cation of magnesium ( $Mg^{2+}$ ). In addition, the 3-vinyl and 13-keto groups exert weak electron withdrawing effects at opposite ends of the Y axis [15]. Figures 1a and b illustrate the fluorescence emission spectrum of chlorophyll **a** in homogeneous and micellar media respectively. In homogeneous medium (DMSO), chlorophyll **a** presented only one band at 680 nm, which is characteristic of the emission of the transition  $S_1 \rightarrow S_0$ . In the presence of polymeric micelles, a reduction in the emission intensity and the presence of three peaks are observed: 513 nm, 550 nm and the maximum at 675 nm.

Static fluorescence anisotropy measurements of chlorophyll **a** in micellar medium were performed using the 433 nm excitation wavelength. The anisotropy was measured at three emission wavelengths providing the

following results: 511 nm,  $A = 0.365$  (G factor = 1.477); 550 nm,  $A = 0.436$  (G factor = 1.421) and 675 nm,  $A = 0.035$  (G factor = 1.726). The higher the anisotropy value implies in a greater restriction on the movement of the probe molecules [16]. Such results may be indicative of a possible association state between the probe molecules at the lower emission wavelengths, in which the anisotropy values are higher. According to the adjustment, chlorophyll **a** presents two lifetimes: the long time has a value of  $\tau_1 = 5.8265$  ns and



(a)



(b)

**Figure 1.** a) Fluorescence emission spectrum of chlorophyll **a** ( $1.0 \times 10^{-5}$  mol.L $^{-1}$ ) in DMSO and b) fluorescence emission spectrum of chlorophyll **a** ( $1.0 \times 10^{-5}$  mol.L $^{-1}$ ) in LUTROL $^{\circledR}$  F127 polymeric micelles (2%). The excitation wavelength used was 433 nm at 25 °C.

represents 95.89% of the decay; the short time has a value of  $\tau_2 = 1.3791$  ns and represents 4.11% of the decay ( $\chi^2 = 1.095$ ). The existence of two values lifetimes can be attributed to the

association of the molecules in micellar medium [17], corroborating with the data of static anisotropy. The time resolved anisotropy measurement was also performed, which provided a rotational correlation time of  $\varphi = 0.1308$  ns (factor  $G = 2.8188$ ).

### 2.3 Association constant

The intensity of chlorophyll **a** emission increased with the addition of the LUTROL solution and there was a small shift of the emission maximum to the region of smaller wavelengths (Figure 2). The increase in intensity is a result of a decrease in the rate of non-radiative decay of the excited state and the displacement indicates a decrease in polarity. To obtain the association constants ( $K_b$ ) of chlorophyll **a** to the polymeric micelles, the fluorescence data were analyzed using the ratio of the inverse of  $\Delta F$  to the inverse of the LUTROL $^{\circledR}$  concentration, according to equation 1 [18]:

$$\frac{1}{\Delta F} = \frac{1}{\Delta F_{\max}} + \frac{1}{\Delta F_{\max}} \frac{1}{K_b} \frac{1}{[\text{LUTROL}]} \quad (1)$$

where  $\Delta F = F - F_0$  and  $\Delta F_{\max} = F_{\max} - F_0$ .  $K_b$  can be determined by the ratio between the intersection and the slope of the obtained line (graph of  $1/\Delta F$  as a function of  $1/[\text{LUTROL}^{\circledR}]$ ). The value for the constant was  $14,4 \text{ M}^{-1}$ .

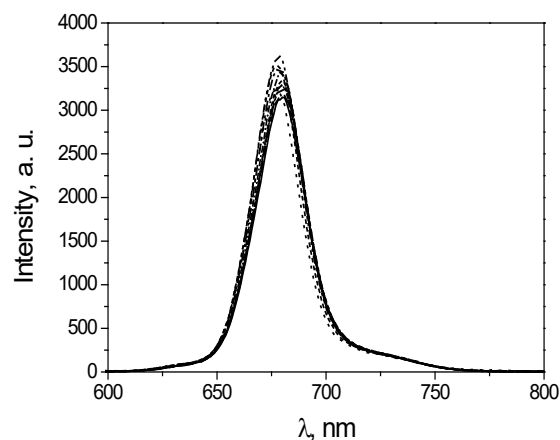


**Figure 2.** Fluorescence emission spectra of chlorophyll **a** ( $1.0 \times 10^{-5}$  mol.L $^{-1}$ ) in DMSO at 25 °C, in the absence (lower curve) and presence (upper curves) of a concentrated solution ( $0.88 \text{ mol.L}^{-1}$ ) of LUTROL $^{\circledR}$  F127. The concentrations of LUTROL ranged between  $(0.44\text{--}17.6) \times 10^{-2}$  mol.L $^{-1}$ .

Coordinated bonds are formed between acids and Lewis bases. A Lewis acid has an unoccupied orbital that can accept a pair of electrons. A Lewis (ligand) base has an unshared electrons pair that are available to be donated to a Lewis acid and form a donor-acceptor complex. Lewis acids and bases are characterized as "soft" or "hard" according to their chemical properties [19]. "Soft" species tend to bind by short-range orbital interactions, whereas hard species interact preferentially by electrostatic forces. The central magnesium atom of chlorophyll **a**, such as a Lewis acid, interacts with proteins through coordination bonds with the side chain of an amino acid as a Lewis base. The compression of the electron cloud in the direction of the Y axis of the chlorophyll **a** molecule, when the C<sub>17</sub>-C<sub>18</sub> double bond and the C<sub>8</sub> vinyl group are reduced, tending to shield the magnesium divalent metallic coordination center (Mg<sup>2+</sup>), effectively reduces the electronic affinity of this metallic center. This results in a weaker interaction with the negative end portion of a fixed dipole or even in the repulsion of negatively charged groups. Water is a Lewis base that appears to be the "regulatory" binder because of its strong interaction with chlorophyll **b** and its poor interaction with chlorophyll **a**. In solution, where water forms hydrogen bonds (dielectric constant, 81), its dipole moment is 2.70 D; in ice, its value is 3.09 D. In an environment in which the dielectric constant has values between 2 to 4, as in a protein or membrane, and possibly in LUTROL<sup>®</sup>, the dipole of a water molecule is probably more close to that in the gaseous phase, 1.85 D. However, when associated with a positive charge such as Mg<sup>2+</sup> in chlorophyll, the dipole moment is probably close to the value of the hydrogen bond. The charge at the negative end of the water dipole provides an electrostatic contribution to the interaction. These factors contribute to the values obtained in the absorption spectra of chlorophyll in the studied systems [20]. The compounds used to interact with chlorophyll **a** as shown in Figure 1 have amide and nitrile groups. These structures interact in various ways with the coordination center of magnesium (Mg<sup>2+</sup>) in the respective chlorophyll by modifying its spectroscopic properties. The compound cypermethrin has 3 oxygen atoms in its structure. On the other hand, the tebutiuron compound has 4 nitrogen atoms, while the hexazinone has 4 nitrogen atoms and 2 oxygen atoms. These compounds interact via

Lewis acid-base interaction with chlorophyll **a**. The pK of an amide is -0.6227, as in the case of tebutiuron, diuron and hexazinone, which may be an indication that electrons in oxygen or nitrogen are not readily available for H<sup>+</sup> binding [19]. However, the group exhibits a relatively strong dipole, with the negative end upon the oxygen atom. The amide side chain in proteins has a dipole moment of 3.46 D. The dipole is strong enough to displace a coordinate water molecule from chlorophyll **a** in the LUTROL environment. In this way, this significant high polar character can generate a representative predisposition to polar intermolecular interactions, favoring the interaction with the water molecule, weakly coordinated to chlorophyll.

Based on the above, chlorophyll **a** can form complexes via magnesium atom (nucleus) with oxygen atoms of various compounds. In organic solvents, this complex is exhibited by the decrease of absorbance at 430 nm in the blue component in the double-blue structure of the blue-violet absorption band in the presence of alcohols, water and oxygen [21]. The presence of LUTROL<sup>®</sup> also provides a microenvironment that allows the interactions between the structures of the compounds and those with the macromolecule as seen in Figures 3a - f. Particularly, polyamines increase the absorbance of chlorophyll **a** at 640 nm, which is indicative of the sixth coordination, as seen in Figures 3a-f around 675 nm. It has recently been reported that when a large displacement occurs (> 10 nm) is indicative of the coordination of two pyridine molecules, while a minor shift, 1-3 nm, indicates the coordination of a single molecule [22]. In the case of Figure 3c, there appears to be a charge transfer complex between chlorophyll and tebutiuron. The apparent band is between 400 and 450 nm.

## 2.4 Steady state fluorescence emission measurements

For chlorophyll **a**, there are two major absorption bands, Soret and Q<sub>y</sub> at 443 and 671 nm, respectively. A weak band, Q<sub>x</sub>, is not well resolved. Fluorescence spectra at 677 nm show a Stokes shift of approximately 132 cm<sup>-1</sup> relative to the Q<sub>y</sub> band. There is another vibronic and resolved band at 737 nm with a relative intensity to the peak of greater than about 15% [19].

Traditionally, the following designations have been made for chlorophyll *a*: 660 nm  $Q_y(0,0)$  and 612 nm  $Q_y(1,0)$ . However, it is suggested that the 612 nm peak of chlorophyll *a* originates from both  $Q_{y1}$  and  $Q_x$ . By analogy, the chlorophyll *b* band is designated at 650 nm at  $Q_y(0,0)$  and at 600 nm at  $Q_y(1,0)$  and probably there is some contribution from  $Q_x$ . These bands have been used as an

index of the coordination state. The Katz group used the ratio of 619-633 nm bands of chlorophyll *a* as an index of the sixth coordination [19]. Under the experimental conditions employed, such bands were not observed. However, the present study indicates similarities with the studies performed for chlorophyll *b* in the presence of spermine.

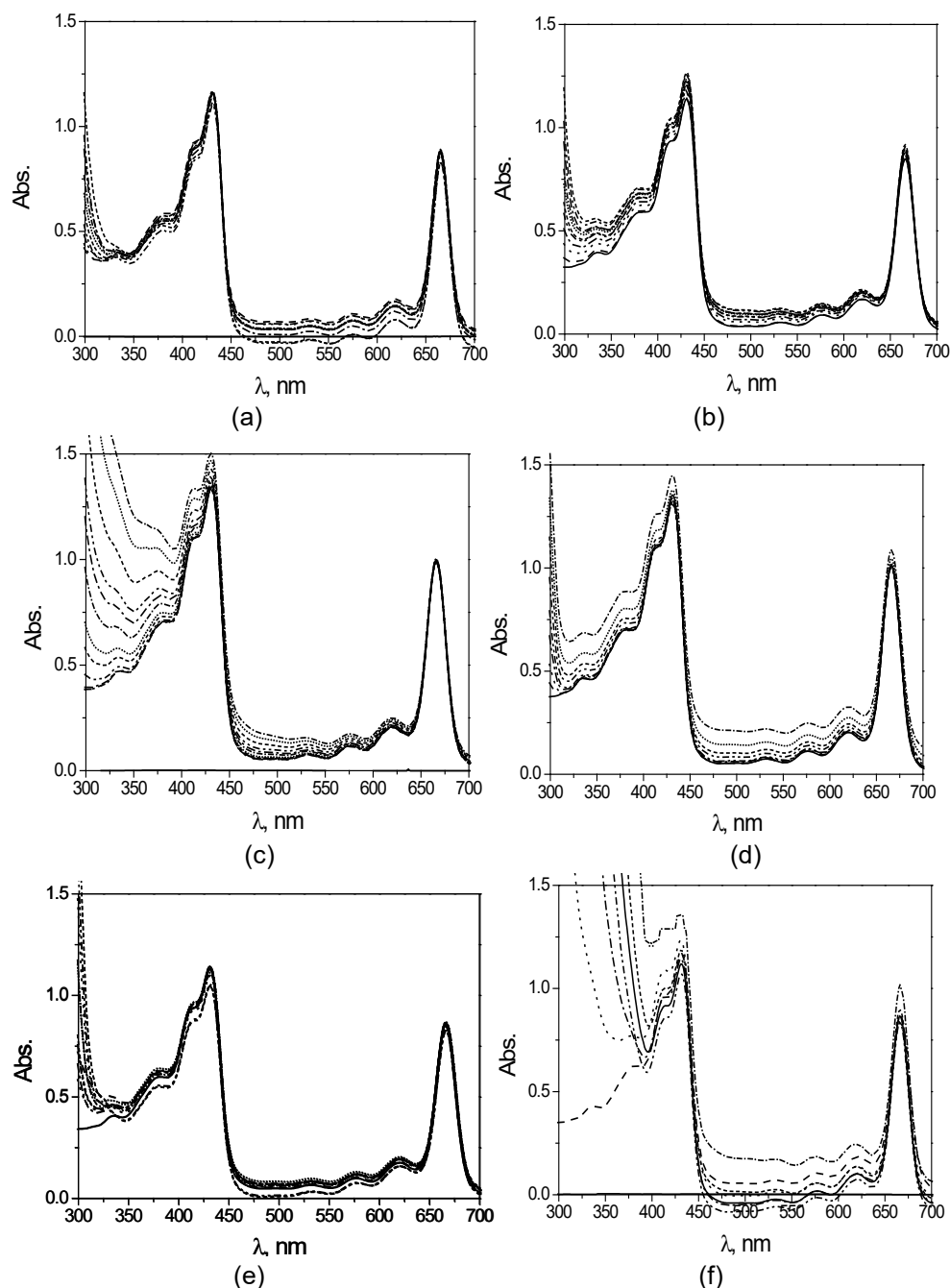
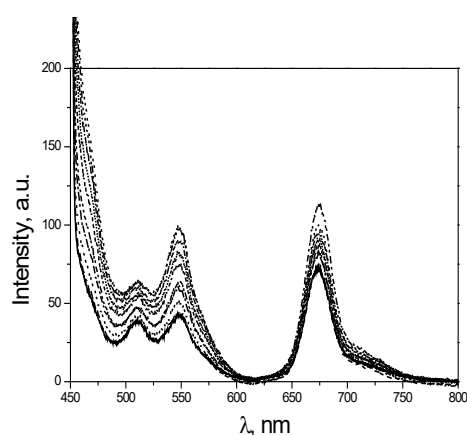


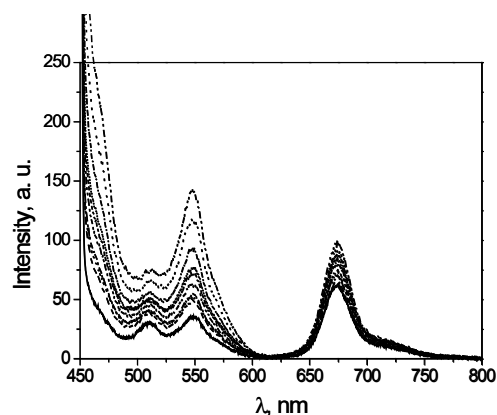
**Figure 3.** Optical absorption spectra of chlorophyll *a* ( $1.0 \times 10^{-5}$  mol.L $^{-1}$ ) in LUTROL® F127 polymeric micelles (2%) at 25 °C, (a) in the absence (lower curve) and presence of cypermethrin (upper curves), (b) in the absence (lower curve) and presence of esfenvalerate (upper curves), (c) in the absence (lower curve) and presence of tebutiuron (upper curves), (d) in the absence (lower curve) and presence of diuron (upper curves), (e) in the absence (lower curve) and presence of hexazinone + diuron (upper curves), and (f) in the absence (lower curve) and presence of methyl-parathion (upper curves).

Some polyamines, such as spermine, appear to extract or displace magnesium from the plane of the ring. In this case, it has two effects on chlorophyll **b** fluorescence (peaks at 640 and 667 nm). Spermine, in particular, increases the chlorophyll **b** fluorescence at 661-667 nm by about 250%. At low concentrations, the fluorescence yield of chlorophyll **b** apparently increased. There is also a slight shift to red at the peak emission of 667 nm. Mg displacement of chlorophyll **b** increases fluorescence and shifts the emission peak (667 nm), while alkaline effects, for example treatment with NaOH, reduces the fluorescence at 662 nm and increases the emission at around 640 nm [21].

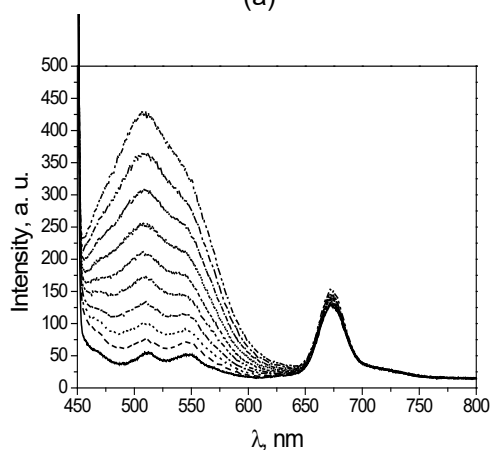
The course of these two effects is illustrated in Figures 4a-i. The insertion of  $Mg^{2+}$  into the ring of chlorophyll **b** produces significant suppression of fluorescence compared to the pigment without  $Mg^{2+}$  [19]. In the case of the compounds used in this work, there is clearly an effect similar to that described above. The effect is more pronounced in the case of tebutiuron, diuron and hexazinone because of the high number of amide groups in their molecular structures. The most exacerbated effect of such behavior is in the case of methyl paration, in which there is an increase in band fluorescence emission around 550 nm and a reduction in band fluorescence emission around 670 nm.



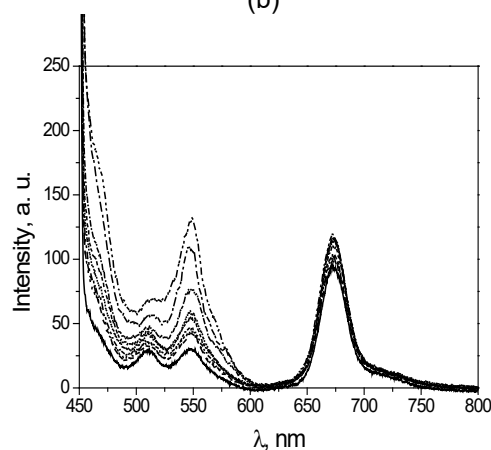
(a)



(b)



(c)



(d)

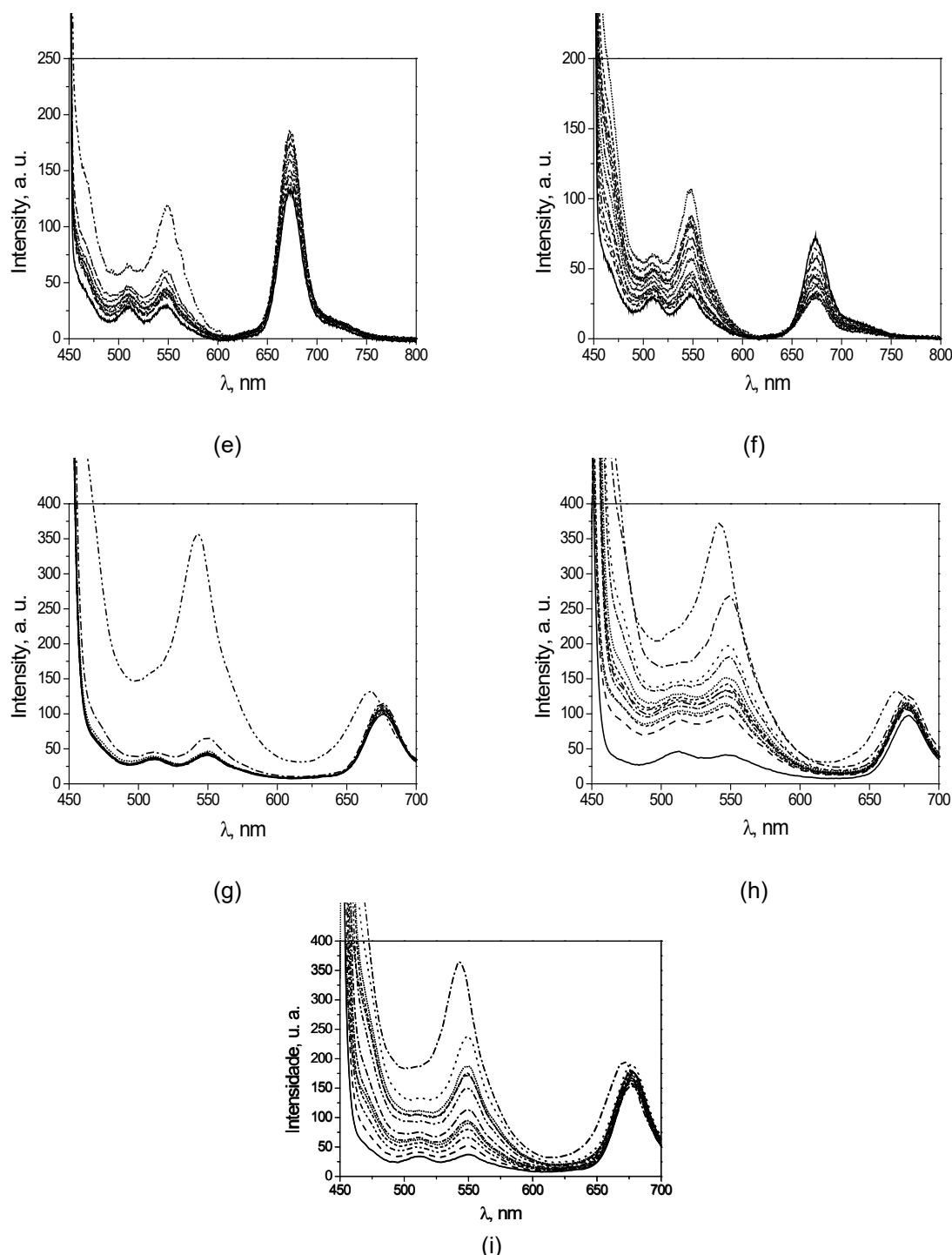


**Figure 4.** Fluorescence emission spectra of chlorophyll **a** ( $1.0 \times 10^{-5}$  mol.L $^{-1}$ ) in polymeric micelles of LUTROL® F127 (2%) at 25 °C, (a) in the absence (lower curve) and presence of cypermethrin (upper curves), (b) in the absence (lower curve) and presence of esfenvalerate (upper curves), (c) in the absence (lower curve) and presence of tebutiuron (upper curves), (d) in the absence (lower curve) and presence of diuron (upper curves), (e) in the absence (lower curve) and presence of hexazinone + diuron (upper curves), (f) in the absence (upper curve) and presence of methyl-parathion (lower curves), (g) in the absence (lower curve) and presence of atrazine (upper curves), (h) in the absence (lower curve) and presence of chlorpyrifos (upper curves) and, (i) in the absence (lower curve) and presence of polytrin (upper curves). The excitation wavelength used was 433 nm.

The axial attachment of chlorophylls to amine ligands is well established, although most studies

do not use chlorophyll **a** and **b**, mainly because of their labile character [19]. In fact, amine ligands



are very stable as axial ligands for most of the complexes that present in the equatorial plane a tetraazamacrocyclic ligand, as the case of porphyrin and chlorin ligands [23]. Therefore, depending on the coordination center, the stability of the axial bonds with nitrogenous ligands tends to be large, especially when the metal center, usually a divalent or trivalent metal cation, exhibits good stability in a configuration with coordination number six, that is, being a hexacoordinated center. In the present work, with the use of absorption and fluorescence spectroscopy, it was verified the possibility of amide groups to coordinate with chlorophyll **a**. Generally, monoamines and monodentate ligands (such as pyridine) coordinate in a simple manner either from one or both sides of the macrocycle. This appears to be the case of the compounds studied. In addition, a ligand with a greater number of interaction sites, such as a tetradentate ligand of short length/size, may interact in a more complex way [19]. This higher complexity of tetraazamacrocyclic ligands, specifically porphyrin ligands or porphyrin derivatives, such as chlorins, has several causal factors, one of the most relevant being the significant flexibility of the porphyrin ring, which can generate a series of spatial conformations Which have been studied in different metalloporphyrins, which has been studied in both metalloporphyrin complexes alone and in heme groups in several hemoproteins [24-28]. In fact, changes in spatial conformation alter substantially the overlapping integrals of the orbital involved, which tends to affect several properties, such as coordination center oxidation state, redox potential, equatorial and axial bond stability, axial ligands, among others.

Spermine reduces the chlorophyll **b** band by 600 nm and increases the band by 635 nm ( $Q_x$ ). By coordinating six  $Q_x$  of chlorophyll **a** there is a shift to 640 nm. According to this view, is evident that when Mg is absent, coordination pairs (640/618 for chlorophyll **a** and 633/600 nm for chlorophyll **b**) are also absent. According to data reported in the literature [19], ring cleavage occurs at higher concentrations of amine. However, more recent contributions have shown that the origin of the emission increase at 640 nm would be related to the coordination state. In all cases, this effect is limiting for the range of amine concentrations for fluorescence studies with 30 mM pigment. In conditions similar to those of chlorophyll **a**, amines

increase the absorbance of chlorophyll **b** around 630 nm suggesting that this type of interaction is also possible for chlorophyll **b**. Such effects (i.e., increase in yield and displacement of the emission peak at 667 nm) occur by removal of the coordination center, i.e. from the  $Mg^{2+}$ . Thus, it has been suggested that  $Mg^{2+}$  was slightly displaced from the ring plane due to coordination with the amines and this, in turn, contributed to the increase in fluorescence yield. Such mechanism of exposure of the metal is exploited by the nature of the prosthetic groups of structure similar to the chlorophyll ring, such as the  $Fe^{2+}$  of the heme (iron-porphyrin) group in the various hemoproteins, such as myoglobin and hemoglobin, which is reinserted in the plane of the ring by oxygen binding [29]. In fact, the spatial conformation acquired by the heme prosthetic group, when the ferrous ion leaves the xy plane, that is, the equatorial plane of the porphyrin ring, is called the doming conformation (doming or domed) [30-33], because the exit of the coordination center, accompanied by the slope of the pyrrolic rings, whose nitrogen atoms are connected to the ferrous center, deforms the spatial arrangement of the heme group, when the iron is pentacoordinated, that is, when the sixth ligands, in this case molecular oxygen in the distal axial position, leaves the first heme coordination sphere [29, 30]. The results of Ioannidis et al. [21] indicate that the complete removal of the magnesium cation increases the fluorescence, which is an expected physico-chemical phenomenon, since the coordination center is the main fluorescence suppressor of the porphyrin systems. Similarly, gradually increasing the  $Mg^{2+}$  shift from the ring plane would significantly increase chlorophyll fluorescence, whereas, reinsertion of that coordination center within a planar array of chlorophyll could suppress fluorescence. A similar behavior is maintained for chlorophyll **a**, but the total suppression capacity is lower under the experimental conditions performed. This suppression mechanism could provide the photosynthetic organism with the ability to activate rapidly (insertion of  $Mg^{2+}$  in the ring will only have a fraction of ms) its photoprotection [19]. In the presence of the methyl-parathion was observed a quenching of chlorophyll **a** emission. The quenching process is described by the Stern-Volmer relation, equation 2 [34]:

$$K_{SV} = \frac{\tau_0 k_q k_- K}{(k_q + k_-)(1 + K[M])} \quad (2)$$

where  $K_{SV}$  is the Stern-Volmer constant,  $K$  is the quenching binding constant given by the ratio of  $k_+/k_-$ , rate constants for exit ( $k_-$ ) and entry ( $k_+$ ) of the quencher from the micelle, the pseudo-unimolecular rate constant ( $k_q$ ) for intramicellar quenching,  $\tau_0$  is the fluorescence lifetime of the probe in the absence of quencher.

The  $K_{SV}$  value was obtained from the angular coefficient of the graph of  $I_0/I$  (using the linear region of the graph), where  $I_0$  and  $I$  are the fluorescence intensities in the absence and presence of quenching, respectively, as a function of the quenching concentration. This graph is shown in Figure 5, in which a downward curvature at higher suppressor concentrations can be observed, indicating that two populations of fluorophores are present; however, only one of them is accessible to the suppressor. This is an indication that in the system formed by chlorophyll **a** and methyl-parathion, the suppression presents the static and dynamic components. The calculated Stern-Volmer constant was  $587 \text{ M}^{-1}$ .

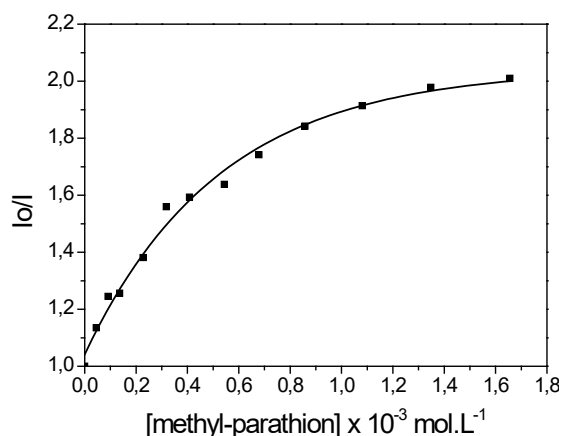


**Figure 5.** Quenching of chlorophyll **a** fluorescence emission ( $1.0 \times 10^{-5} \text{ mol.L}^{-1}$ ) in LUTROL® F127 polymeric micelles (2%) at  $25^\circ \text{C}$  in the presence of methyl-parathion.

## 2.5 Time resolved fluorescence measurements

The agrochemical-chlorophyll **a** combination is formed at low concentrations of agrochemicals and involves the formation of complex or aggregate between different molecules. This

association usually leads to quenching of probe fluorescence. The quenching process depends on the structure of the agrochemical and its concentration, which will directly affect the probability of agrochemical-chlorophyll **a** encounter. It has been shown that addition of agrochemical affects the state of aggregation of the complex. It is important to note that this effect was more pronounced in smaller complexes, rather than larger complexes, again highlighting its possible key role in non-photochemical quenching. One explanation is that the addition of any agrochemical (low or high energy  $S_1$ ) to isolate complexes may disadvantage the chlorophyll-chlorophyll interactions observed at low pH (responsible for quenching), resulting in increased chlorophyll fluorescence, i.e. anti-quenching. For sufficiently low energy  $S_1$  agrochemicals, this effect will compete with its ability to quenching chlorophyll fluorescence by singlet-singlet deexcitation. It has been previously suggested that these compounds can actually act as "anti-quenchers" by preventing chlorophyll-chlorophyll interactions. Such behavior has recently been demonstrated in organic solvents for the suppression of chlorophyll fluorescence, when addition of agrochemicals initially disaggregates chlorophyll, resulting in increased fluorescence [14, 35, 36]. In the present work, fluorescence decays (Figures 6a, b and c and Table 1) revealed an efficient interaction between chlorophyll **a** and methyl-parathion. In the case of esfenvalerate, there is practically no quenching of dynamic fluorescence. The decays suggest that energy migration may be occurring through Forster's mechanism and there is also the possibility of association of the molecules in the LUTROL® micro-environment, which have a non-emissive behavior. It should be noted that there are two main components in the chlorophyll **a** decay profile, one very fast, in a smaller proportion and one slower, in greater proportion.

Data from the profile analysis of the decay curves of chlorophyll **a** in micellar medium in the absence and presence of herbicides are shown in Table 1. The fluorescence decays were evaluated using reconvolution analysis, which considers decay measurement and instrumental response, according to the equation 3:

$$Fit = A + \alpha_1 e^{\left(\frac{-t}{\tau_1}\right)} + \alpha_2 e^{\left(\frac{-t}{\tau_2}\right)} + \alpha_3 e^{\left(\frac{-t}{\tau_3}\right)} + \alpha_4 e^{\left(\frac{-t}{\tau_4}\right)} \quad (3)$$

where  $\alpha_1$ ,  $\alpha_2$ ,  $\alpha_3$  and  $\alpha_4$  are pre-exponential factors;  $\tau_1$ ,  $\tau_2$ ,  $\tau_3$  and  $\tau_4$  are lifetimes; and A is a constant. This model is provided from software package of Edinburgh Analytical Instruments.

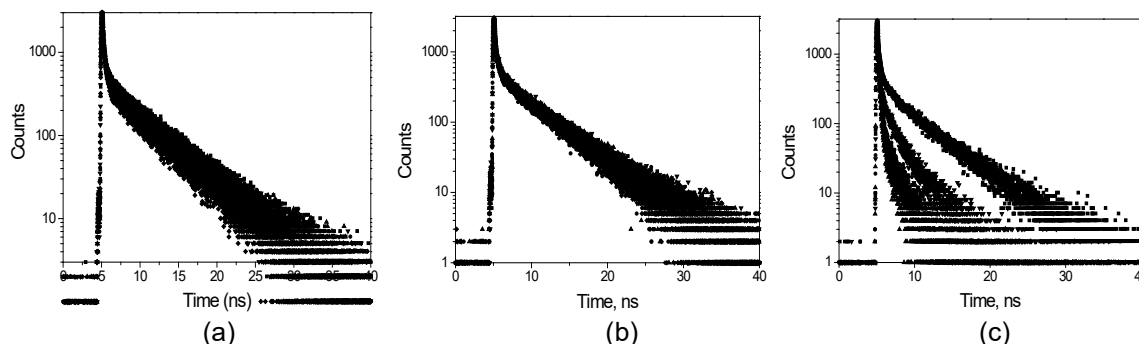


**Figure 6.** Chlorophyll **a** fluorescence ( $1.0 \times 10^{-5}$  mol.L $^{-1}$ ) decays in LUTROL $^{\circledR}$  F127 polymeric micelles (2%) varying the concentration of agrochemicals at 25 °C, (a) in the absence (upper curve) and presence of cypermethrin (lower curves), (b) in the absence (upper curve) and presence of esfenvalerate (lower curves) and, (c) in the absence (upper curve) and presence of methyl-parathion (lower curves).

**Table 1.** Profile analysis of chlorophyll **a** fluorescence decays ( $1.0 \times 10^{-5}$  mol.L $^{-1}$ ) in LUTROL $^{\circledR}$  F127 polymeric micelles (2%) at 25 °C.

[cypermethrin] ( $\times 10^{-4}$ mol.L $^{-1}$ )	$\tau_1$ (ns)	$\tau_2$ (ns)	B $_1$	B $_2$	$\chi^2$	$\langle \tau \rangle$ (ns)
0	5.6336	1.0369	432.672	156.901	1.112	5.3460
0.291	5.4589	0.8132	386.781	161.220	1.107	5.1873
0.871	5.3906	0.4726	395.589	364.654	1.088	5.0229
1.736	5.2859	0.4555	348.985	372.107	1.083	4.8794
2.882	5.1721	0.4038	309.588	448.303	1.129	4.6879
[esfenvalerate] ( $\times 10^{-5}$ mol.L $^{-1}$ )	$\tau_1$ (ns)	$\tau_2$ (ns)	B $_1$	B $_2$	$\chi^2$	$\langle \tau \rangle$ (ns)
0	5.1417	0.3235	493.966	946.410	1.134	4.7499
0.238	5.1947	0.3404	499.961	793.324	1.225	4.7375
0.712	5.2663	0.4426	481.464	717.746	1.171	4.7292
1.419	5.1752	0.3247	477.813	860.556	1.180	4.6827
2.356	5.2046	0.3867	452.710	797.546	1.152	4.6470
3.517	5.0977	0.3353	436.473	933.607	1.150	4.5221
[methyl-parathion] ( $\times 10^{-3}$ mol.L $^{-1}$ )	$\tau_1$ (ns)	$\tau_2$ (ns)	B $_1$	B $_2$	$\chi^2$	$\langle \tau \rangle$ (ns)
0	4.8571	0.3939	422.041	809.288	1.136	4.2564
0.911	3.2996	0.2723	341.940	769.352	1.104	2.7435
2.728	2.8365	0.3682	210.433	266.972	1.209	2.4875
5.439	2.4498	0.2539	189.020	723.652	1.128	1.8260
9.030	2.0346	0.2382	144.025	662.843	1.062	1.4056

$\langle \tau \rangle$  is the mean value of  $t$  and obtained according to equation 6.  $\chi^2$  is a fitting based on Marquardt-Levenberg algorithm.

The collisional fluorescence quenching is described by the Modified Stern-Volmer equation, equation 4 [37]:

$$\frac{I_0}{I} = 1 + k_q \tau_0 [Q] = 1 + K_D [Q] \quad (4)$$

The data shows that methyl-parathion exhibited a more efficient dynamic quenching. Using the equation 3 the quenching rate constant value was estimated:  $k_q = 8.46 \cdot 10^9$  M $^{-1}$  s $^{-1}$ . The value of  $k_q$  may reflect the quenching efficiency or the fluorophore accessibility to the quencher. The

meaning of this constant can be understood in terms of the frequency of collisions between freely diffusing molecules.

### 3. Material and Methods

For all the fluorescence and optical absorption measurements quartz cuvette with 10 mm path length were used. The fluorescence emission measurements were carried out by using a Hitachi

F-7000 model spectrometer with a xenon excitation light source with a temperature controlled sample holder. The steady state anisotropic measurements were carried out in the presence of polarized filter. The absorption spectra were obtained by using a UV-Vis Shimadzu (model 1650) spectrophotometer.

In Figure 7 are shown the chemical structures of the agrochemicals used.

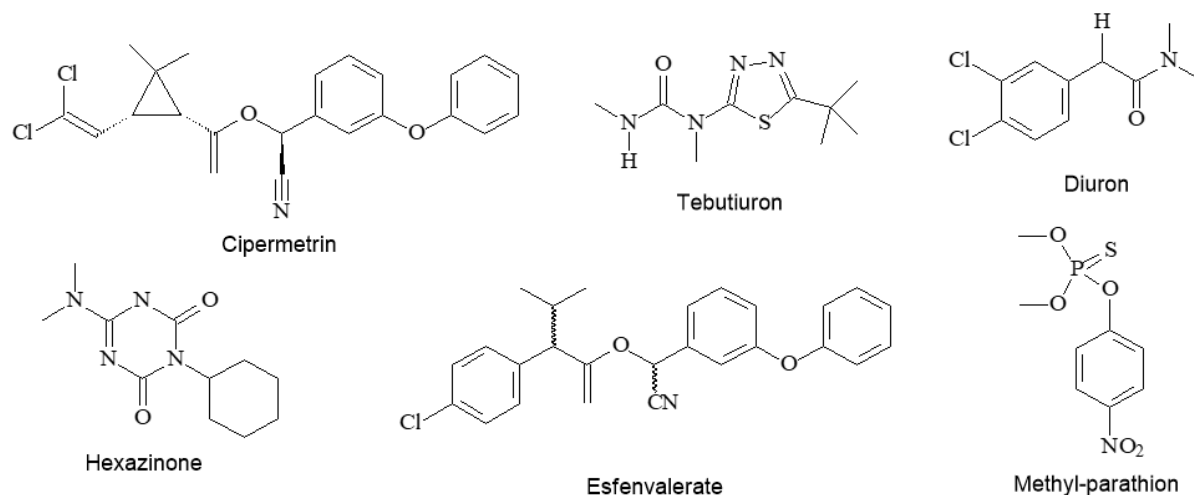


**Figure 7.** Structures of compounds used to interact with chlorophyll a.

The fluorescence decays were obtained using the single photon counting method. A Spectra Physics spectrometer operating with a pulsed Tsunami 3950 titanium-sapphire laser beam with a power of 6.0 to 10.0 watts was used. The laser beam pulse frequency was modulated by a Pulse Picker (model 3986, Spectra Physics), which generates pulsed laser beam in the wavelength of 840-1000 nm. A laser beam pulse selector and a first and second harmonic generator were used to control the repetition pulse frequency and to obtain the laser radiation wavelength needed, respectively. In the specific case of chlorophyll was used a second harmonic with excitation at 440 nm. The excitation laser pulses were time correlated with the sample emission fluorescence pulses and these measurements were carried out by using an Edinburgh Instruments spectrometer, which contains a temperature controlled sample holder. For the anisotropic decay measurements a Babonet-Soleil BSC (Halbo Optics) compensator in the excitation beam and a Glan-Tompson prism polarizer (P920, Edinburgh Instruments) in the emission beam were used

[38]. A software provided by Edinburgh Instruments was used to analyze the individual decays, which were fitted to multi-exponential curves (equation 5) [39]:

$$I(t) = \sum_i \alpha_i e^{\left(\frac{-t}{\tau_i}\right)} \quad (5)$$

where  $\alpha_i$  are the pre-exponential factors and  $\tau_i$  are the lifetimes. The quality of the fit was judged by the analysis of the statistical parameters reduced- $\chi^2$  and by the inspection of the residuals distribution. Mean lifetimes were calculated from intensity weighted lifetimes according to equation 6:

$$\langle \tau \rangle = \frac{\sum \alpha_i \tau_i^2}{\sum \alpha_i \tau_i} \quad (6)$$

where  $\tau_i$  and  $\alpha_i$  are lifetime and pre-exponential factor of the component  $i$  of the decay.

The chemicals, acetone (Aldrich), chlorophyll **a** (Aldrich), clopirifos (Sabre Agro Science 45%), dimethyl sulfoxide (Merck), LUTROL® F127 (BASF), methanol (Aldrich), pyrene (Aldrich), polytrin (Syngenta – cipermethrin 40/L + profenefos 400 g/L) were used as received. The cipermethrin (Pika Pau, 4.8 %), tebutiuron (Combine, 50 %), diuron (Nortox, 50 %), a mixture of diuron (53.3 %) and hexazinone (6.7 %) (Jump Milenia), esfenvalerate (Sumidan, 25 %) were dissolved in acetone and then the solution was filtered through a 0.2 µm cellulose membrane. The methyl-parathion (Agripec, 60 %) was dissolved in methanol and then the solution was filtered through a 0.2 µm cellulose membrane.

#### 4. Conclusions

Fluorescence measurements showed that chlorophyll **a** is associated with LUTROL® F127 polymeric micelles. In the spectroscopic studies of chlorophyll **a** in micellar medium in the presence of agrochemical molecules, there is an increase in the intensity of absorption and in the emission. The increase in fluorescence emission is probably related to the displacement of the magnesium atom from the porphyrin ring. In the specific case of the compound tebutiuron, the emission spectra indicated the possibility of formation of a charge transfer complex with chlorophyll **a**. The methyl-parathion was the only one to have a static fluorescence quenching of chlorophyll **a** at the main peak (~ 674 nm).

Time-resolved fluorescence measurements provided two lifetimes for chlorophyll **a** in the absence and in the presence of the agrochemicals. This behavior may be related to the possibility of association states of the probe molecules. The data with temporal resolution were performed in the presence of the compounds: cypermethrin, methyl-parathion and esfenvalerate. With the addition of cypermethrin and methyl-parathion, a reduction in the chlorophyll lifetime was observed, but the decrease in the lifetime values were more accentuated in the presence of methyl-parathion. This behavior evidences the presence of the dynamic quenching process. In the case of esfenvalerate, it was not observed a variation of the lifetime with the increase of the concentration of this compound, which indicates that in this case

does not occur the quenching process.

#### Acknowledgments

Thanks are due to the Brazilian Research Agencies CNPq (474019/2012-8) and CAPES. The authors thank to Prof. Dr. Amando S. Ito (FFCLRP-USP) for the time-resolved measurements and Prof. Dr. Rodrigo F. Bianchi (DEFIS-UFOP) for the steady-state measurements.

#### References and Notes

- [1] Streit, N. M.; Canterle, L. P.; do Canto, M. W.; Hecktheuer, L. H. H. *Cienc. Rural.* **2005**, *35*, 748. [\[Crossref\]](#)
- [2] Lanfer-Marquez, U. M. *Rev. Bras. Cienc. Farm.* **2003**, *39*, 227. [\[Crossref\]](#)
- [3] Pavlović, D.; Nikolić, B.; Đurović, S.; Waisi, H.; Anđelković, A.; Marisavljević, D. *Pestic. Phytomed.* **2014**, *29*, 21. [\[Crossref\]](#)
- [4] Malmsten, M.; Lindman, B. *Macromolecules* **1993**, *26*, 1282. [\[Crossref\]](#)
- [5] Kwon, G. S.; Kataoka, K. *Adv. Drug Delivery Rev.* **1995**, *16*, 295. [\[Crossref\]](#)
- [6] Van Domeselaar, G. H.; Kwon, G. S.; Andrew, L. C.; Wishart, D. S. *Colloids Surf. B.* **2003**, *30*, 323. [\[Crossref\]](#)
- [7] Teixeira, S. C. G.; Canela, M. C. *Quim. Nova.* **2007**, *30*, 1830. [\[Crossref\]](#)
- [8] Chaim, A.; Botton, M.; Scramin, S.; Pessoa, M. C. P. Y.; Sanhueza, R. M. V.; Kovaleski, A. *Pesqui. Agropecu. Bras.* **2003**, *38*, 889. [\[Crossref\]](#)
- [9] Consolin Filho, N.; Leite, F. L.; Carvalho, E. R.; Venancio, E. C.; Vaz, C. M. P.; Mattoso, L. H. C. *J. Braz. Chem. Soc.* **2007**, *18*, 577. [\[Crossref\]](#)
- [10] Oliveira, R. T. S.; Machado, S. A. S. *Quim. Nova* **2004**, *27*, 911. [\[Crossref\]](#)
- [11] Konrad, M. L. F.; Silva, J. A. B.; Furlani, P. R.; Machado, E. C. *Bragantia* **2005**, *64*, 339. [\[Crossref\]](#)
- [12] Váradi, G.; Darkó, E.; Lehoczki, E. *Plant Physiol.* **2000**, *123*, 1459. [\[Crossref\]](#)
- [13] Cassana, F. F.; Lima, C. S. M.; Falqueto, A. R.; Bacarin, M. A.; Braga, E. J. B.; Peters, J. A. *Revista Brasileira de Biotecnologia* **2007**, *5*, 867.
- [14] Kalyanasundaram, K.; *Photochemistry in Microheterogeneous Systems*, Orlando: Academic Press, 1987.
- [15] Hooper, J. K.; Eggink, L. L.; Chen, M. *Photosynth. Res.* **2007**, *94*, 387. [\[Crossref\]](#)
- [16] Romani, A. P.; Marquezin, C. A.; Soares, A. E. E.; Ito, A. S. *J. Fluoresc.* **2006**, *16*, 423. [\[Crossref\]](#)
- [17] Nakamura, K.; Kowaki, T.; Scully, A. D.; Hirayama, S. *J. Photochem. Photobiol. A: Chem.* **1997**, *104*, 141. [\[Crossref\]](#)

- [18] Tabak, M.; Borissevitch, I. E. *Biochim. Biophys. Acta* **1992**, *1116*, 241. [\[Crossref\]](#)
- [19] Jensen, W. B. *Chem. Rev.* **1978**, *78*, 1. [\[Crossref\]](#)
- [20] Dinoiu, V.; Vasilescu, M.; Latus, A.; Lungu, L. *Rev. Chim.* **2011**, *62*, 396.
- [21] Goncharova, N. V.; Goldfeld, M. G.; Chetverikov, A. G.; Binyukov, V. I. *Photosynthetica* **1997**, *34*, 77. [\[Crossref\]](#)
- [22] Ioannidis, N. E.; Tsiavos, T.; Kotzabasis, K. *Photochem. Photobiol.* **2012**, *88*, 98. [\[Crossref\]](#)
- [23] Lindoy, L. F.; Chemistry of Macrocyclic Ligand Complexes, Cambridge: Cambridge University Press, 1989.
- [24] Walker, F. A. *Coord. Chem. Rev.* **1999**, *185-186*, 471. [\[Crossref\]](#)
- [25] Moreira, L. M.; Ribelatto, J. C.; Imasato, H. *Quim. Nova.* **2004**, *27*, 958. [\[Crossref\]](#)
- [26] Walker, F. A. *Chem. Rev.* **2004**, *104*, 589. [\[Crossref\]](#)
- [27] Ilari, A.; Bonamore, A.; Farina, A.; Johnson, K. A.; Boffi, A. *J. Biol. Chem.* **2002**, *277*, 23725. [\[Crossref\]](#)
- [28] Walker, F. A.; Benson, M. J. *Phys. Chem.* **1982**, *86*, 3495. [\[Crossref\]](#)
- [29] Niedzwiedzki, D. M.; Blankenship, R. E. *Photosynth. Res.* **2010**, *106*, 227. [\[Crossref\]](#)
- [30] Perutz, M. F.; Wilkinson, A. J.; Paoli, M.; Dodson, G. G. *Annu. Rev. Biophys. Biomol. Struct.* **1998**, *27*, 1. [\[Crossref\]](#)
- [31] Spiro, T. G.; Burke, J. M. *J. Am. Chem. Soc.* **1976**, *98*, 5482. [\[Crossref\]](#)
- [32] Rakshit, G.; Spiro, T. G. *Biochemistry* **1974**, *13*, 5317. [\[Crossref\]](#)
- [33] Spiro, T. G.; Stong, J. D.; Stein, P. *J. Am. Chem. Soc.* **1979**, *101*, 2948. [\[Crossref\]](#)
- [34] Romani, A. P.; Vena, F. C. B.; Nassar, P. M.; Tedesco, A. C.; Bonilha, J. B. S. *J. Colloid Interface Sci.* **2001**, *243*, 463. [\[Crossref\]](#)
- [35] Kupper, H.; Dedic, R.; Svoboda, A.; Hála, J.; Kroneck, P. M. H. *Biochim. Biophys. Acta* **2002**, *1572*, 107. [\[Crossref\]](#)
- [36] Young, A. J.; Frank, H. A. *J. Photochem. Photobiol. B.* **1996**, *36*, 3. [\[Crossref\]](#)
- [37] Lakowicz, J. R. Principles of Fluorescence Spectroscopy, New York: Springer, 2011
- [38] Alonso, L.; Mendanha, S. A.; Marquesin, C. A.; Berardi, M.; Ito, A. S.; Acuña, A. U.; Alonso, A. *Int. J. Pharm.* **2012**, *434*, 391. [\[Crossref\]](#)
- [39] Romani, A. P.; Ito, A. S. *Biophys. Chemist.* **2009**, *139*, 92. [\[Crossref\]](#)